



Finite-element analysis method to ensure the safety of invisible capping beams reinforced via the quick-replacement method

Shuai Tian, Bo Sun, & Luyang Zhang

School of Civil Engineering, Liaoning University of Science and Technology, Anshan 114 051, China

Received: 17 March 2021; Accepted: 27 August 2021

This paper presents a Finite-Element Analysis (FEA) method to solve the problem of reduced bridge safety due to insufficient durability of invisible capping beams. To reinforce a C30 invisible capping beam effectively and reasonably, a quick-repair replacement concrete reinforcement method was utilized, and the strength necessary for the appropriate admixture assessed. Specifically, the bearing capacity of the reinforced capping beam was studied via a single-point loading test, and the optimal replacement thickness required to install the beam within two days and restore normal operation within three days was determined using the non-linear software package MIDAS FEA. A finite-element model of equivalent size was employed using MIDAS FEA to obtain the deflection, tensile stress, and pressure stress at the boundary. The results indicate that C40 early strength concrete with 0.1–0.2% sodium gluconate admixture has the appropriate properties to achieve the target. It can be used to replace deteriorated concrete on the surface of invisible capping beams with a replacement rate of 30%. Further, to achieve the goal of resuming traffic within three days, the analysis results indicate that bilateral replacement with thickness 2×10 cm is optimal and the maximum replacement thickness should not exceed 2×20 cm.

Keywords: Bridge engineering, Pier structure, Safe maintenance, MIDAS/FEA, Replacement method

1 Introduction

Overpasses are designed to relieve traffic pressure and minimize the use of construction land while ensuring the rapid development of cities and growth of national economies. Considering longitudinal traffic capacity, clearance, and structural appearance, invisible capping beams have been incorporated into overpass designs. However, it is impossible to determine early defects in invisible capping beams because of their characteristic invisibility. In particular, snow removal with salt spilling in the northern areas of China results in surface concrete erosion and peeling; meanwhile, the corrosion of the reinforcement bars accelerates the damage to the invisible capping beam. The single-pier-type invisible capping beam is often used at the junction of two ramps to ensure a smooth and aesthetically pleasing upper structure. Therefore, it is necessary to renovate and reinforce invisible capping beams to increase the service life of an urban overpass.

To reinforce capping beams, Zhao *et al.*¹ studied vertical cracks on strengthened double-column concrete capping beams and provided related measures for maintenance and reinforcement. They

also suggested steps for subsequent maintenance. Yazdani *et al.*² studied the reinforcement effect of anchored and pre-saturated carbon fiber-reinforced polymer laminated boards on concrete bridges, providing another reference for bridge reinforcement. Chin *et al.*³ studied the reinforcement effect of steel-plate covering on concrete, and subsequently established the effectiveness of this method for concrete strengthening. Gookin *et al.*⁴ renovated and reinforced three severely damaged concrete columns by replacing the concrete, covering it with carbon fiber sheets, and adding a steel hoop. The results indicated that the columns reinforced using this replacement method achieved the optimal effect. Norris *et al.*⁵ reinforced four concrete piers damaged after repetitive loading, using the concrete replacement method. Their results indicated that the reinforced component showed considerably improved compressive resistance and ductility; however, the stiffness of the component was slightly reduced under simulated seismic excitation of the bridge pier. Zhang *et al.*⁶ analyzed the defects of invisible capping beams in the Ya-Yuan overpass and reinforced the beams using the steel-plate covering method, thereby providing a reference for reinforcing an invisible capping beam. However, studies on the reinforcement

of invisible capping beams remain limited. Although the steel-plate covering method can be used for this purpose, it affects the structural appearance and also cannot eliminate the corrosion of the internal steel bars in an invisible capping beam.

There is a dearth of finite-element simulation analysis research on the damage and reinforcement of invisible capping beams. Existing studies are predominantly focused on beam and pier reinforcement,⁷⁻⁸ concrete damage,⁹ and the performance of the interface between the reinforcement materials and concrete.¹⁰

This paper presents a finite-element analysis (FEA) method that solves the problem of reduced bridge safety due to insufficient durability of invisible capping beams, which are used as an alternative to steel-plate reinforcement. The proposed method was developed through investigation,¹¹⁻¹³ experiments, and analysis. Because an invisible capping beam is a part of the structure of an urban overpass, the surface-degraded concrete and corroded steel bars can be renovated quickly without considerably affecting urban traffic; this concept is inspired by the rapid renovation and construction conducted in the case of the San Yuan Bridge in Beijing, China. In this study, C40 early strength concrete was used as the replacement and reinforcement material for a C30 concrete invisible capping beam. The bearing capacity of the reinforced capping beam was studied via a single-point loading test. The optimal replacement thickness required to install the beam within two days and restore normal operation within three days was determined using the MIDAS FEA finite-element modeling software. The relationship between the bending resistance and replacement area for the invisible capping beam was established based on the existing design theory for reinforcement and the experimental results. Thus, this study can provide guidance for fast renovation of invisible capping beams, enabling a return to normal overpass operation within three days.

First, we analyzed the basic theory and method of renovating an invisible capping beam with concrete from the perspective of established standards. Second, material performance and repair beam loading tests were performed based on the concept of rapid repair. Then, using the test data, finite-element simulation analysis was performed. Finally, based on the test data and simulation results, the main construction points for the rapid repair of invisible capping beams were determined.

2 Materials and Methods

2.1 Fundamental theory

According to GB 50367-2013,¹⁴ if an invisible capping beam is reinforced using the replacement method, the bearing capacity of the normal section is affected by the concrete replacement depth for the compressive zone.

(1) If the concrete replacement depth for the compressive zone is $h_1 \geq x$, the bearing capacity of the normal section of the invisible capping beam is calculated as per the strength grade of the replaced concrete, in accordance with GB 50010-2010.¹⁵

(2) If the concrete replacement depth for the compressive zone is $h_1 < x$, the bearing capacity of the normal section of the invisible capping beam is calculated as

$$\gamma_0 M_d \leq f_c b h_1 h_{01} + f_{c0} b (x - h_1) h_{00} + f_{cd} A'_s (h_0 - a'_s)$$

$$f_c b h_1 + f_{c0} b (x - h_1) = f_{sd} A_s - f_{cd} A'_s$$

where f_c is the design value of the compressive strength of the replacement concrete; f_{c0} is the design value of the compressive strength of the original member concrete; x is the height of the compressive zone of the reinforced concrete; h_1 is the displacement depth of the concrete in the compression zone; h_0 is the sectional effective height; h_{01} is the distance from the resultant force point of the longitudinal tensile reinforcement to the centroid of the replacement concrete; and h_{00} is the distance from the resultant point of the longitudinal tensile reinforcement to the centroid of the original concrete ($x - h_1$).

Further more, f_{sd} and f_{cd} denote the designed tensile strength and compressive strength, respectively, of the longitudinal bars in the invisible capping beam (MPa); A_s and A'_s represent the sectional areas of longitudinal bars in the tensile zone and compressive zone, respectively; and b , a'_s , γ_0 , and M_d denote the width of the rectangular section, the distance between the resultant force point of the longitudinal compressive bars and the proximal edge of the section, an important structural coefficient, and the designed bending moment, respectively.

Erosion on the top and sides of the beam structure caused by substances such as chloride ions results in damage to the invisible capping beam, as shown in Fig. 1. Therefore, it is impossible to strengthen the invisible capping beam structure using only replaced concrete for the compressive zone. To overcome this problem, based on the increased-section

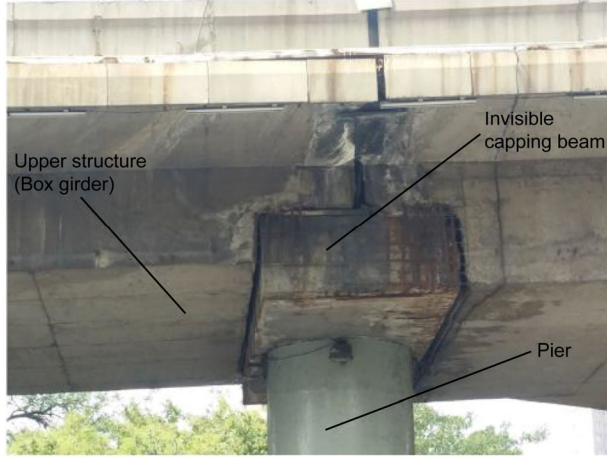


Fig. 1 — Common defects of invisible capping beam.

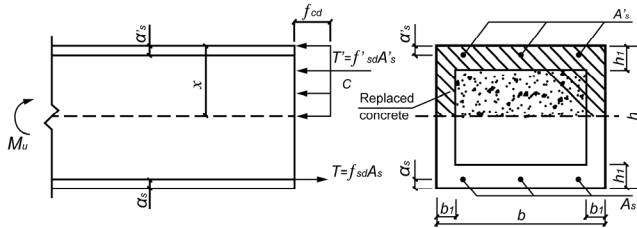


Fig. 2 — Sectional view of replacement for invisible capping beam.

strengthening-related calculation in JTGT522-2019¹⁶ and the replacement and strengthening features of the invisible capping beam, a method is provided for replacing the concrete in the compressive zone and U-shaped zone on both sides of the beam without changing the original structure size or altering the structural appearance. Fig. 2 shows the replacement section when the invisible capping beam is strengthened using the replaced-concrete strengthening method.

Figure 2 indicates that if the section of double bars on the beam is strengthened with the replaced concrete, the bearing capacity of the normal section can be calculated as

$$\text{where } C=f_{c0}(b-2b_1)(x-h_1)+f_c[bh_1+2b_1(x-h_1)]$$

Because the internal force at the horizontal direction of the section is zero, i.e., $T+C+T'=0$,

$$f_{c0}(b-2b_1)(x-h_1)+f_c[bh_1+2b_1(x-h_1)]+f'_{sd}A'_s=f_{sd}A_s$$

The moment is calculated for the resultant force point T shown in Fig. 2. According to the force balance conditions for the invisible capping beam,

$$\gamma_0 M_d \leq M_u = \{f_{c0}(b-2b_1)(x-h_1)+f_c[bh_1+2b_1(x-h_1)]\} [(h_0-\frac{x}{2})+f'_{sd}A'_s(h_0-a'_s)]$$

Similarly, the moment is calculated for another resultant force point T' shown in Fig. 2. According to the force balance conditions for the invisible capping beam,

$$\gamma_0 M_d \leq M_u = -\{f_{c0}(b-2b_1)(x-h_1)+f_c[bh_1+2b_1(x-h_1)]\} [(\frac{x}{2}-a'_s)+f_{sd}A_s(h_0-a'_s)]$$

where b_1 , h_1 , and x denote the real width of both ends of the replaced concrete on the beam (mm), the height of both ends of the replaced concrete on the beam (mm), and the height of the compressive zone with concrete strengthening, respectively.

For the invisible capping beam reinforced using the replaced-concrete strengthening method, the shear capacity of the original and replaced-concrete bonding surfaces must satisfy

$$\gamma_0 V_d \leq 0.12 f_{cd} b h_0 + 0.85 f_{sv} \frac{A_{sv}}{S_v} h_0$$

where b , f_{sv} , A_{sv} , and S_v denote the widths of the new and old concrete bonding surfaces (mm), the designed tensile strength of the embedded steel bars on the original and replaced-concrete bonding surfaces (MPa), the total cross-sectional area of the embedded steel bars on the original and replaced-concrete bonding surfaces (mm²), and the space between the embedded steel bars (mm), respectively.

In practice, the degrees of external erosion on the top and sides of the invisible capping beam are larger than those on the bottom. Furthermore, the replaced concrete on the top has almost no influence on the bending resistance, owing to the negative bending moment. Because the replaced concrete on the bottom is thin, its influence on the bending resistance can be neglected. In addition, the influence of the maintenance time required for replacing the concrete on the bearing capacity of the invisible capping beam is not considered in the theoretical calculation. Therefore, the design requirements for the invisible capping beam cannot be satisfied to ensure quick resumption of normal overpass operation. In this study, the bearing capacity was investigated to determine whether it can satisfy the design requirements for quick resumption of normal operation of the overpass when renovating the concrete on both sides of the invisible capping beam; this investigation was conducted via experiments and finite-element modeling based on on-site conditions. Furthermore, the relationship between the replacement

zone and bending resistance of the invisible capping beam when using only replacement concrete on both sides of the invisible capping beam was determined based on the experimental results and theoretical analysis.

2.2 Materials

a) Cement: Grade 42.5 rapid-drying and rapid-hardening sulfoaluminate cement (R·DFC) was used. Based on the experimental results, its performance satisfies the related requirements.

b) Fine aggregate: River sand with a fineness modulus of 2.89 was used. According to the standard,¹⁷ its performance satisfies the related requirements.

c) Coarse aggregate: Gravel made from unique limestone with 5–25 mm continuous grading in Liaoning was used. According to the standard,¹⁷ its performance satisfies the related requirements.

d) Admixture: Sodium gluconate (NG) was used as a special admixture¹⁸ for preparing early strength concrete; this product cannot corrode steel bars. Instead, it can increase the setting time for R·DFC and delay or prevent the hydration of C₃A and C₃S. It has no significant influence on the later-stage hydration reaction or the strength of concrete.

2.3 Performance test for materials

2.3.1 Appropriate admixture test

According to the literature¹⁹ and the results of a performance test, the optimal amount of NG and the optimal mortar mix proportion ($m_c:m_w:m_s = 1:0.36:1.5$) were determined for experiments, based on the mortar strength and setting time under different amounts of NG admixture (0, 0.1%, 0.2%, and 0.3%). (For the mortar, m , subscripts: C=cement, W=water, S=sand.) The 70.7 mm × 70.7 mm × 70.7 mm mortar component for the test was prepared and maintained for 6 h and 28 h under the standard conditions for demolding. A compression machine with a defined loading speed of 0.25 kN/s was used for the loading test; it was controlled through a computer operation interface.

2.3.2 Strength test for hardened concrete

1) Test of compressive strength: According to the test methods for cement and concrete used in highway engineering, the mix proportion of the concrete is determined preliminarily based on an empirical formula involving the related parameters; the proportion is $m_c:m_w:m_s:m_g = 472:170:598:1160$. A total of 84 test models with dimensions of 100 mm × 100 mm × 100 mm were prepared and then placed in

a maintenance box at a temperature of 20 ± 2 °C and relative humidity of 95%. The maintenance times for the 6 h- and 12 h-aged models were 5 h and 11 h, respectively. The test was performed once after demolding; however, the remaining models were maintained until the stipulated time. Moreover, a compression testing machine with a maximum pressure of 3000 kN and a loading speed of 0.8 MPa/s was used to measure the compressive strength of concrete under maintenance times of 6 h, 12 h, 1 d, 3 d, 7 d, 14 d, and 28 d for NG admixture amounts of 0%, 0.1%, 0.2%, and 0.3%.

2) Test of splitting strength: The same test devices were used; the models were numbered after demolding as per the amount of NG admixture. The test of splitting tensile strength for conducted as per the relevant age of the test specimen, and the loading speed during the test was set to 0.05 MPa/s. Special splitting tensile molds, arc-shaped steel blocks with a diameter of 150 mm, steel supports, and the aforementioned molds were used to prepare a total of 84 test specimens. The splitting strengths of the concrete were measured under the maintenance times of 6 h, 12 h, 1 d, 3 d, 7 d, 14 d, and 28 d for the NG admixture amounts of 0, 0.1%, 0.2%, and 0.3%.

2.3.3 Design for mix proportion of concrete

A comparison of the aforementioned results indicates that the optimal amount of NG admixture varies from 0.1% to 0.2%. Therefore, the optimal amount was set to 0.15% in this study. According to related studies,^{20–23} concrete strength increases faster for water/cement ratios of ≤ 0.3 . Therefore, the water/cement ratio was set to 0.3 for this test. The mix proportion for the C40 early strength concrete was $m_c:m_w:m_s:m_g:NG = 533:160:580:1127:1.5\%$.

2.4 Single-point loading test for concrete beam

Based on the loading features of the invisible capping beam and on similarity theory, an original beam, L1, with C30 concrete and two partially renovated beams, L2 and L3, with C30 concrete were designed. Beams L2 and L3 were renovated with the prepared C40 early strength concrete in the aforementioned test. Table 1 summarizes the details of the test.

1) Design of test beams: Based on the structure of the invisible capping beams in the Wu-Yi Road Overpass in Anshan City, China, three test beams were designed to represent the invisible capping beam on a scale 1:4, in accordance with similarity theory and the conditions for the laboratory loading device.

Table 1 — Test details

Beam	L1	L2	L3
Type	Original beam with C30 concrete	Renovated beam	Renovated beam
Process	Loading after maintenance for 56 d.	Renovating rest sections after maintenance for 28 d for some sections of the original beam, and loading after the maintenance for 28 d.	Renovating rest sections after maintenance for 54 d for some sections of the original beam, and for loading after maintenance for 2 d.
Role	L2 and L3 benchmark component	L1 comparison component; L3 benchmark component	L1 and L2 comparison component

L1, beam no. L1; L2, beam no. L2; L3, beam no. L3

Table 2 — Load at the first oblique crack on test beams (kN)

Beam	Original concrete	Replaced concrete
L1	220	—
L2	235	230
L3	225	210

L1, beam no. L1; L2, beam no. L2; L3, beam no. L3

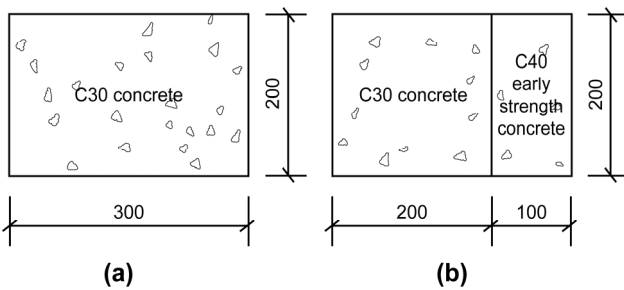


Fig. 3 — Section form of the test beam (mm).

Figure 3 presents the sectional size of three test beams, which were 1400 mm in length. L1 denotes the original beam with C30 concrete, while L2 and L3 are the renovated beams. The reinforcement was provided at the rectangular section of the double-steel bars.

Consolidation between the beam body and pier was achieved by simulating a 300 mm × 150 mm pier along the length direction of the rectangular beam. To facilitate a comparative analysis on the beam casting and the stress between the replaced and original concrete, renovation with a depth of 100 mm was provided on a single side of the beam body. The reinforcements of the three renovated test beams were completely identical. Figure 4 shows the reinforcement diagram. Grade HRB335 was selected for the main reinforcement, and Grade HPB235 was selected for the hoop; furthermore, the strength of the steel bars was consistent with the requirements in practice.

Preparation of test beams: The beam body was poured laterally twice in different mixed-proportions of the raw materials. The original beam with the common concrete was poured first. L1 was poured

completely and then directly maintained for 56 d in accordance with the relevant standards; however, L2 and L3 were poured partially. The surface erosion depth of the invisible capping beam in an actual bridge is over 10 cm, and the total erosion area reaches 30% of the sectional area. To achieve 30% replacement for the test beams, the first batch of pouring was implemented for 200 mm of concrete at the end of the test beam to simulate the original concrete. Then, maintenance was performed for 28 d in accordance with the standards. The second batch was poured performed after the maintenance of the first batch of concrete. Thus, the remaining sections of L2 and L3 were renovated with concrete. The code for strengthening requires that the depth of the replaced concrete be at least 60 mm. Considering concrete vibrations, the second batch of concrete was poured to a depth of 100 mm to simulate the replaced concrete. The maintenance times were 28 d for L2 and 2 d for L3. The loading test was conducted after the maintenance of the test beams. Figure 5 shows the process of preparing the test beams.

Loading of test beams: A single static loading was conducted for the three test beams using the single-point loading method, as shown in Fig. 6. A 50 T compression testing machine was used as the loading device. In the test, the loading mode was “automatic control,” the load control rate was 0.200 kN/s, and the displacement control rate was 0.300 mm/s. The test ended when the load reached the defined value. In Fig. 7, the loading force P represents the support force of the single-column pier, while the counterforce of the two supports represents the vertical force transmitted to the invisible capping beam through the foundation support from the upper single-box beam. Figure 7 shows the loading diagram of the test beams.

Detection for the test beams: A XL2101B6 static strain indicator was used to measure the strain of the steel bar and the strain, deflection, load, crack width, and crack distribution of the concrete.

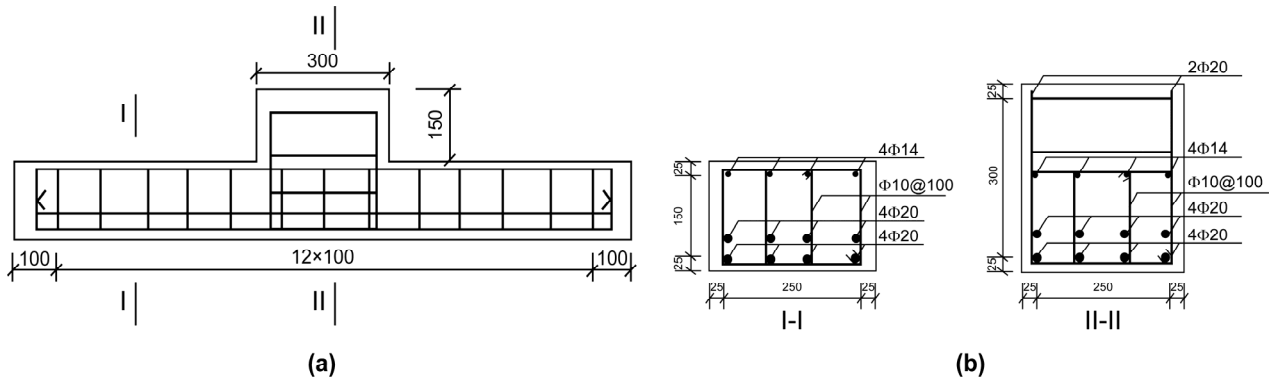


Fig. 4 — Reinforcement diagram of test beams (mm) (a) side reinforcement, and (b) sectional reinforcement.



Fig. 5 — Process of preparing test beams (a) embedment of steel reinforcement cage in template, and (b) pouring of the first batch of concrete.



Fig. 6 — Loading for test beams.

2.5 Finite-element modeling

MIDAS FEA is a non-linear analysis software package developed by professionals and experts in the field of civil engineering, with assistance and coordination from TNO DIANA BV. This software is designed for civil engineering applications. A model with a size equivalent to that of the test beams was

built in MIDAS FEA. The simulated support had dimensions of 300 mm × 50 mm × 20 mm. In addition, the surfaces were subjected to applied pressures of 230 kN and 500 kN, respectively, to simulate the normal operation condition and limit state of the bearing capacity, respectively.

Based on the analysis results for boundary deflection, tensile stress, and pressure stress, the optimal thickness was obtained by comparing the renovation thicknesses of 5 cm, 10 cm, and 15 cm under the maintenance durations of 2 d, 7 d, and 14 d, respectively, for the renovated beams. Figure 8 shows the grid-partition model of the finite elements and steel bar units. The size of the unit grid is 10 mm.

In Fig. 8, concrete is simulated using solid elements, and reinforcement is simulated by truss elements. The concrete and reinforcement elements share nodes. The material models of the concrete and reinforcement were respectively selected from the GB(RC) and GB(S) databases included in the software. Super-high early strength cement (RS) was selected for the C40 concrete, and ordinary cement or early strength cement (N,R) was selected for the C30

concrete. Bonding between the new and old concrete was realized with Interface Element such that there is very little damage to the plasticity.

3 Results and Discussion

3.1 Analysis for appropriate admixture test

Figure 9 shows the setting time and compressive strength of mortars with different amounts of NG. The amount of NG is the ratio between high-efficiency water reducing the retarder and R·DFC.

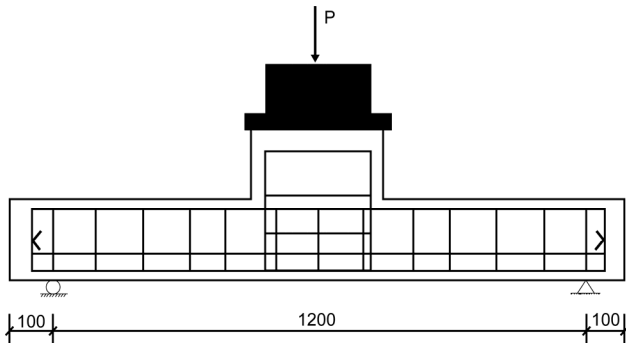


Fig. 7 — Loading diagram of test beams (mm).

According to the analysis, the appropriate amount of NG admixture varies from 0.1% to 0.2%. Mixing with NG can reduce the early strength of the mortar. However, the appropriate amount of NG admixture can improve the subsequent strength of the mortar. If the amount of NG admixture is 0.1–0.2%, the setting time of the mortar is appropriate for normal construction.

3.2 Analysis for hardening strength

Figure 10 shows the experimental results for the compressive strength and splitting tensile strength of concrete with different amounts of NG admixture.

Figure 11 shows that with 0–0.3% NG admixture, the compressive strength declines by 149.58% within 6 h. This can be attributed to the increased amount of NG admixture, which delays the induction period of C₃S and the hydration reaction of the cement, as well as reduces the early compressive strength of the concrete. However, for 0–0.2% NG admixture, the compressive strength increases by 15% within 3 d. The compressive strength measured with 0.1% NG is similar to that with 0.2% NG. Furthermore, when the

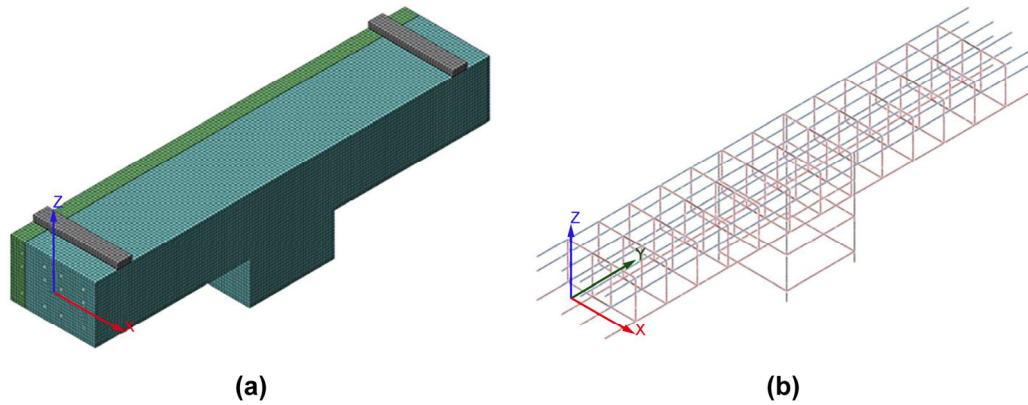


Fig. 8 — Finite-element model (a) grid partition and (b) steel bar unit.

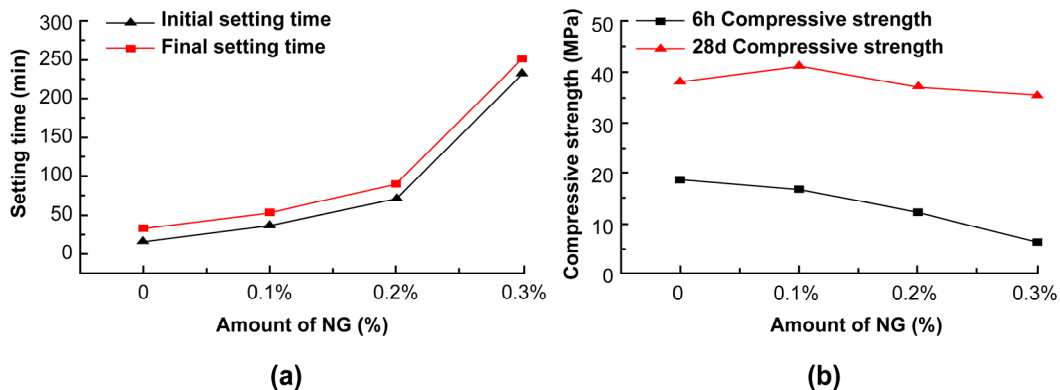


Fig. 9 — Setting time and compressive strength of mortar with different amount of NG (a) setting time of mortar with different amounts of NG, and (b) compressive strength of mortar with different amounts of NG.

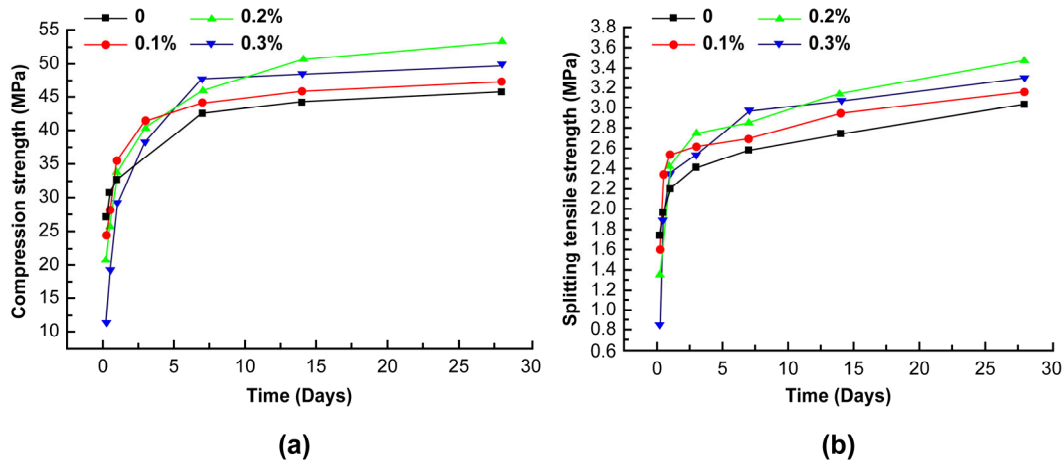


Fig. 10 — Compressive strength and splitting tensile strength of concrete with different amounts of NG admixture (a) compression strength of concrete with different amounts of NG admixture and (b) splitting tensile strength of concrete with different amounts of NG admixture.

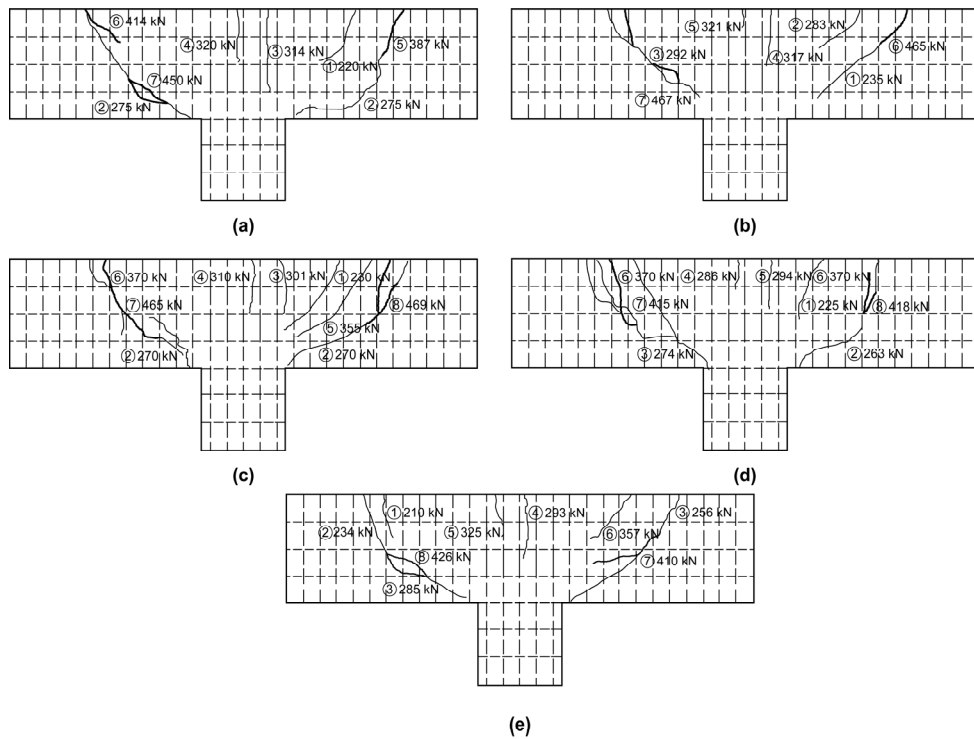


Fig. 11 — Distribution diagram of cracks (a) expanded view of crack on L1, (b) expanded view of crack on non-renovated side of L2, (c) expanded view of crack on renovated side of L2, (d) expanded view of crack on non-renovated side of L3, and (e) expanded view of crack on renovated side of L3.

amount of NG admixture is 0.2–0.3%, the compressive strength declines by 5%. When the amount of NG admixture is 0.2%, the compressive strength reaches 53.21 MPa within 28 d. As shown in Fig. 12, when the amount of NG admixture is 0, the splitting strength increases by 28.89% within 6–12 h and by 3.28% within 14–28 d. When the amount of

NG admixture is 0.2%, the splitting strength increases by 64.03% within 6–12 h and by 11.42% within 14–28 d. According to the analysis based on the normal operation of an overpass 3 d after strengthening the invisible capping beams with the replaced concrete, the appropriate amount of NG admixture is 0.1–0.2%.

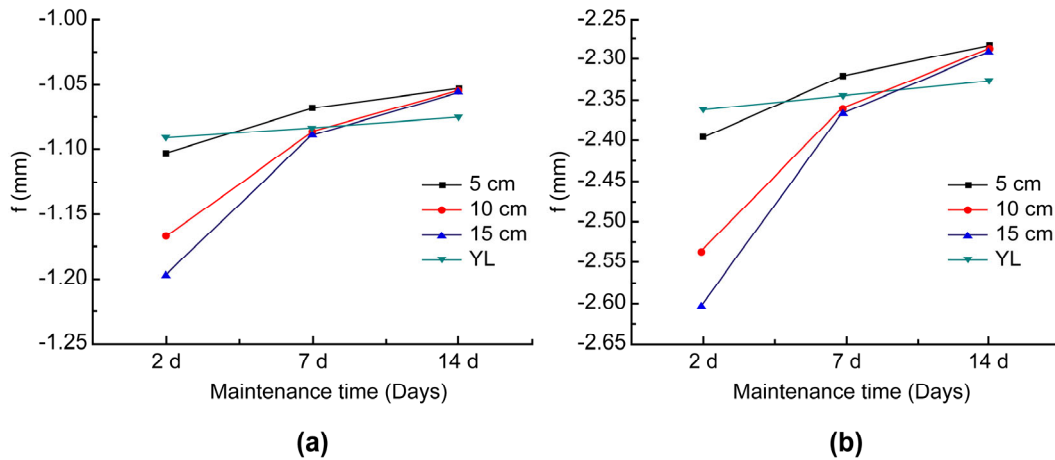


Fig. 12 — Maximum deflection at upper boundary of invisible capping beam (mm) (a) normal operation condition, and (b) limit state.

3.3 Analysis for single-point loading test

1) Comparison of the first oblique crack: To compare and analyze the cracking performance on the oblique section of the replaced concrete for the test beam, the first diagonal cracks are summarized as follows.

As listed in Table 2, the loads at the first oblique cracks on the sides with the original concrete for L1, L2, and L3 are the same. The load at the first oblique crack on the concrete renovation side of L3 is slightly lower than the corresponding loads for L1 and L2. This indicates that the early tensile strength of the early strength concrete is slightly low. However, the load at the first oblique crack on L2 is larger than that on L1 and L3. This indicates that the later-stage strength of the early strength concrete is large.

Comparison of bearing capacity: Fig. 11 shows the distribution of cracks with loading on the component. The crack diagram is plotted based on the actual conditions of the invisible capping beam with the bridge pier on bottom.

Figure 11 shows that multiple parallel oblique cracks and concrete slugs appeared at the failure position of the three test beams. They resulted from shear failure, which is related to the effective constraint on the growth of oblique cracks from the longitudinal load-bearing steel bars and hoops on the test beams. Multiple oblique cracks formed in the middle (about 350 mm) of the span between the two ends. As the load continued to increase, one of the cracks transformed into a critical oblique crack. Subsequently, the load continued to increase while the oblique crack expanded to the bottom of the base plate until the concrete at the top of the crack was compressed and damaged. Compared with those on

the original beam L1, cracks on the non-renovated side of L2 expanded less, while those on the renovated side of L2 were distributed densely; the overall cracking load of L2 was higher than that of L1. This is related to the enhancement in the later-stage overall bearing capacity of the renovation side via strengthening using C40 concrete. Compared with those on L2, the cracks on L3 expanded more, which may be related to the shorter maintenance time for the C40 concrete on the renovated side. However, the overall cracking load on L3 was approximately the same as that on L1. As a result, restoration of normal overpass operation within 3 d can be achieved; however, the passage of heavy vehicles through the overpass must be limited.

Therefore, restoration of normal overpass operation within 3 d can be achieved by strengthening the invisible capping beams using the proposed replacement method. Moreover, the limit bearing capacities are 450 kN, 469 kN, and 426 kN for L1, L2, and L3, respectively; these values are higher than the vertical loading forces inversely computed using the bending resistance of the rectangular section of the double-steel bars and the shear capacity of the oblique section of test beams, as per the existing standard equations. Moreover, the effectiveness of the renovation satisfies the requirements for the bearing capacity of the structure.

3.4 Analysis for finite-element modeling

1) Comparison of maximum deflection (f) at the upper boundary of the invisible capping beam: Fig. 12 shows the maximum deflection at the upper boundary of the invisible capping beam. *YL* denotes the deflection of the original beam without renovation.

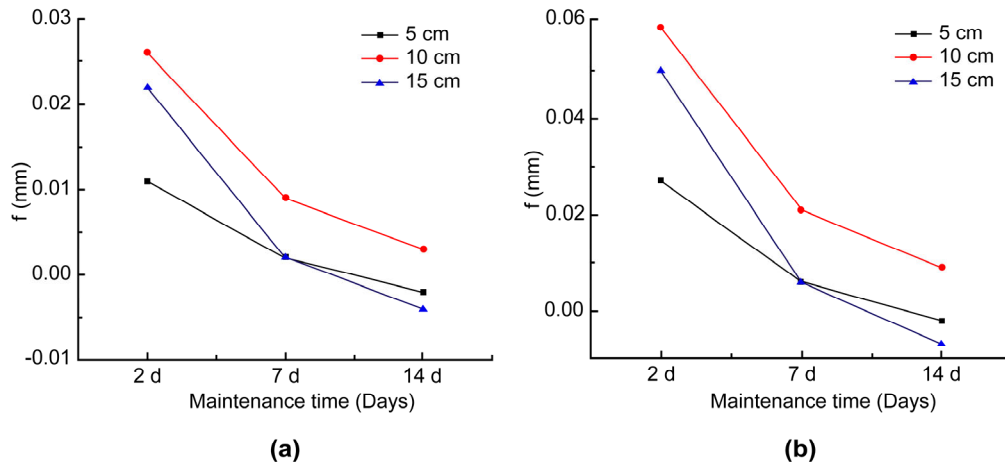


Fig. 13 — Relative deformation of maximum deflection between renovated beam and original beam (mm) (a) normal operation condition, and (b) limit state.

Figure 12 shows that when the thickness of the renovated part is 5 cm, the maximum deflection of the renovated beam is approximately the same as that of the non-renovated beams. When the maintenance time for the renovated part is 2 d out of the total 30 d maintenance time, the deformation of the deflection increases substantially with the thickness of the renovated part. This may be because the thicker concrete replaced within 2 d is not dried completely. When the maintenance time for the renovated part is 7 d out of the total 35 d maintenance time, the deformation of the deflection for the renovated beam is consistent with that for the original beam. When the maintenance time for the renovated part is 14 d out of the total 42 d maintenance time, the deformation of the deflection for the renovated beam is significantly lower than that for the original beam. This indicates that the later strength of the early strength concrete after the renovation is high, which corroborates the results of the single-point loading test. Therefore, based on the result analysis, the appropriate thickness for the renovation is 5 cm when the requirement of restoring normal operation of the overpass is satisfied. Because the test beams are designed as per a scale of 1:4, the appropriate thickness for both sides should be 2×10 cm.

Comparison of the relative deformation of the maximum deflection (f) at the upper boundary of the invisible capping beam: Fig. 13 shows the deformation of the maximum deflection (f) at the upper boundary of renovated side of the beam compared with that at the non-renovated side.

Figure 13 shows that the deformation of the deflection for the renovated part is consistent with

that for the non-renovated part. When the maintenance time for the renovated part is 2 d, the deformation of the renovated part with a thickness of 5 cm is closer to that of the nonrenovated part. When the maintenance time for the renovated part is 14 d, the relative deformation is negative, i.e., the deformation of the renovated part of the beam is lower than that of the non-renovated part. This can be attributed to the improved strength of the renovated part with C40 concrete, which results in lower deformation than that in the original beam, which is composed of C30 concrete. Based on the aforementioned results, the optimal thickness for renovating invisible capping beams using the replacement method is 5 cm (2×10 cm for both sides in practical engineering applications).

Comparison of primary stress at the boundary of the invisible capping beam: As shown in Figs 14 and 15, the tensile and compressive stresses at the upper and lower boundaries of the capping beam are extracted when the replacement thicknesses (n) are 5 cm, 10 cm, and 15 cm, the concrete maintenance times (t) for the renovated parts are 2 d, 7 d, and 14 d (denoted with n - t d in the figures), and the maintenance times (t) for the original beams (YL) are 30 d, 35 d, and 42 d (denoted as YL - t d in the figures). Figure 14 shows the tensile stress (σ_t) at the upper boundary of the beam. Fig. 15 shows the compressive stress (σ_c) at the lower boundary of the beam. There is a 100-mm interval between the upper and lower boundaries of the capping beam.

Figures 14 and 15 indicate that the stress at the boundary positions decreases in the order following orders (i) original beam > 15 cm > 10 cm > 5 cm

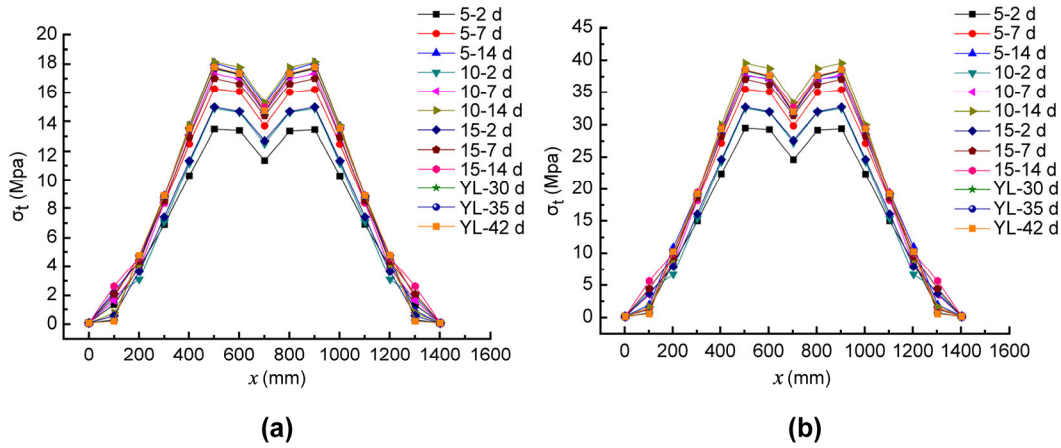


Fig. 14 — Compressive pressure at lower boundary of invisible capping beam (MPa) (a) normal operation condition, and (b) limit state.

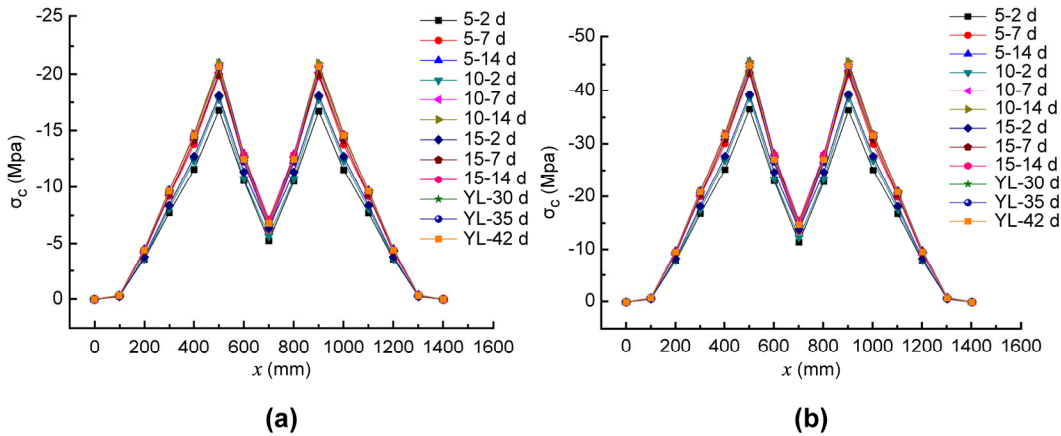


Fig. 15 — Tensile stress at upper boundary of invisible capping beam (MPa) (a) normal operation condition, and (b) limit state.

when the maintenance time for the renovated beam is 2 d, (ii) original beam > 10 cm > 15 cm > 5 cm when the maintenance time for the renovated beam is 7 d, and (iii) 10 cm > 5 cm > original beam > 15 cm when the maintenance time for the renovated beam is 14 d. When the maintenance time for the renovated beam is 14 d (maintenance time for original beam is 42 d) and the thicknesses are 10 cm and 5 cm, respectively, the stress curve is similar to that of the original beam. When the thickness of the renovated part reaches 15 cm, the stress at the boundary position is lower than that in the original beam, and the requirements and standards for the renovation cannot be met. Therefore, when the invisible capping beam is renovated using the replacement method, the maximum thickness should not exceed 10 cm.

3.5 Relationship between replacement zone and bending resistance

Based on the previously mentioned fundamental theory of structural design for invisible capping

beams and the experimental data reported herein, the relationship between the replacement zone and bending resistance of the invisible capping beam is summarized herein as a reference for strengthening design, as shown in the equation below:

$$\frac{M_u}{M_{u0}} = 1 + \frac{0.7A_n}{A} \left(\frac{f_c}{f_{c0}} - 1 \right)$$

where M_u , M_{u0} , A_n , A , f_c , and f_{c0} denote the bending resistance of the invisible capping beam after strengthening, bending capacity of the invisible capping beam before corrosion, area of the replacement zone on both sides of the section of the invisible capping beam, sectional area of the invisible capping beam, designed compressive strength of the concrete for replacement, and designed compressive strength of the original concrete on the invisible capping beam, respectively.

4 Conclusion

The conclusions drawn from this study are as follows:

Using 42.5-grade double-fast sulfoaluminate cement and 0.1–0.2% NG as an admixture, early strength concrete for repairing C30 invisible capping beams can be prepared.

This early strength concrete can be used to replace deteriorated concrete on the surface of invisible capping beams with a replacement rate of 30%. The replacement-reinforced invisible capping beam can enable restoration of normal traffic within three days, but it is necessary to limit the passage of heavy vehicles.

According to the finite-element modeling, when the thickness for renovation is 5 cm, the thickness for both sides is 2×10 cm in practical engineering. At this value, the obtained strength of the renovated beam is basically close to that of the original beam, which satisfies the requirement for returning normal operation of the overpass. The overpass can be opened to drivers completely when the maintenance time reaches 14d.

On the premise of restoring normal traffic within 3 days, the actual repair thickness of the invisible capping beam should be 2×10 cm on both sides, and the actual engineering repair thickness should not exceed 2×20 cm on either side.

In this study, one side of the invisible capping beam was selected for the reinforcement test and simulation analysis; this differs from actual structure-reinforcement situations. This is a limitation of this study. In follow-up research, we intend to perform reinforcement tests and simulation analyses of invisible capping beams from the perspective of the core beam, to ensure that the reinforcement of the structure will be closer to that in an actual situation.

Acknowledgements

This work was supported by the scientific research project of Liaoning Education Department (2020LNJC02) and the Excellent Talents training project of Liaoning University of Science and Technology (2019RC01).

References

- 1 Zhao Q, & Wang C, *J Highway Transport Res Develop (Appl Technol Ed)*, 9 (2018) 259.
- 2 Yazdani N, Aljaafreh T, & Beneberu E, *Compos Struct*, 235 (2020) 111733.
- 3 Chin C L, Ma C K, Tan J Y, Ong C B, Awang A Z, & Omar W, *Constr Build Mater*, 211 (2019) 919.
- 4 Lehman D E, Gookin S E, Nacamuli A M, & Moehle J P, *ACI Struct J*, 98 (2001) 233.
- 5 Norris T, Saadatmanesh H, & Ehsani M R, *J Struct Eng*, 123 (1997) 903.
- 6 Zhang H, *Guangdong Arch Civil Eng*, 1 (2012) 57.
- 7 Daud S A, Daud R A, & Al-Azzawi A A, *Ain Shams Eng, J* 12 (2021) 31.
- 8 Daud S A, Forth J P, & Nikitas N, *Eng Struct*, 163 (2018) 267.
- 9 Wu Y, & Peng K, *Finite element-smearred crack combined algorithm based bridge corbel analysis* (IOP Conference Series: Earth and Environmental Science), 2018, 189, 022017.
- 10 Mazzotti C, & Murgio F S, *Compos Part B-Eng*, 75 (2015) 212-225.
- 11 Han H, *China Standardization*, 4 (2017) 187.
- 12 Liwei S, *Damage analysis for capping beam system on main piers of a certain bridge and strengthening construction*, Master's Thesis, Xi'an University of Architecture and Technology, Xi'an, 2012.
- 13 Wei H, *Research on the technology of renovating locally defective concrete with displacement method*, Doctoral Thesis, Chongqing University, Chongqing, 2015.
- 14 GB 50367-2013, Code for reinforcement design of concrete structures. China Communication Press, 2013
- 15 GB 50010-2010, Code for design of concrete structures. China Communication Press, 2010
- 16 JTJ T522-2019, Code for design of highway bridge reinforcement. China Communication Press, 2019
- 17 JTG E42-2005, Test methods of aggregate for highway engineering. China Communication Press, 2005
- 18 JT/T 523-2004, Concrete admixtures for highway engineering. Ministry of Communication of China, 2004
- 19 Yong K, *Research on influences of sodium gluconate on setting and hardening of cement paste*, Master's Thesis, Huazhong University of Science and Technology, Wuhan, 2009.
- 20 Fang J, *Research on preparation of super-early strength cement-based materials and their performances*, Doctoral Thesis, Southeast University, Nanjing, 2015.
- 21 Sharma A, Duraimurugan S, & Vasugi V, *IOP Conf Ser Mater Sci Eng*, 431 (2018) 042009.
- 22 Dai M, Qin L, & Liu Y, *IOP Conf Ser Mater Sci Eng*, 245 (2017) 032022.
- 23 Lee S, Nguyen N, Le T S, & Lee C, *Int J Concr Struct Mater*, 10 (2016) 257.